



University of Pennsylvania
ScholarlyCommons

Master of Chemical Sciences Capstone
Projects

Department of Chemistry


5-5-2020

Monolayer Self-Assembly of Monodisperse Nanocrystals at The Liquid-Air Interface

Di An

University of Pennsylvania, andi1@sas.upenn.edu

Follow this and additional works at: https://repository.upenn.edu/mcs_capstones

 Part of the [Chemistry Commons](#)

An, Di, "Monolayer Self-Assembly of Monodisperse Nanocrystals at The Liquid-Air Interface" (2020).
Master of Chemical Sciences Capstone Projects. 29.
https://repository.upenn.edu/mcs_capstones/29

This paper is posted at ScholarlyCommons. https://repository.upenn.edu/mcs_capstones/29
For more information, please contact repository@pobox.upenn.edu.

Monolayer Self-Assembly of Monodisperse Nanocrystals at The Liquid-Air Interface

Abstract

The study of nanocrystals (NCs) self-assembly into monolayers have attracted significant interests, due to wide applications in sensors, catalysts, nanodevices and pattern transfer. Liquid-air interface self-assembly (LAISA) is a useful technique used for the monolayer fabrication. In this capstone project, a library of NCs is built for LAISA and binary superlattice study. Monodisperse iron oxide, gold and gadolinium fluoride NCs of various sizes were synthesized by modifying reported methods.^{9,10,20} The obtained NCs were characterized by TEM, SAXS, DLS and TGA, revealing their geometry, size and surface chemistry. The second part of this project is optimizing conditions of LAISA. Significant variables, including evaporation rate, NCs geometry, and ambient environment were isolated and studied for different building blocks. Centimeter-scale NCs monolayers with long-range order were obtained by using optimized conditions of LAISA. The binary superlattice system of spherical NCs was also investigated during this project with optimized LAISA. A 1:2 number ratio of iron oxide to gold NCs was used to fabricate binary superlattice monolayers by LAISA. The structure was revealed with TEM. However, future work is needed to investigate other size ratio and number ratio of two different kinds of NCs, and their effects on 2D structures.

Keywords

nanocrystals monolayers, liquid-air interface self-assembly, binary superlattice

Disciplines

Chemistry

Creative Commons License



This work is licensed under a [Creative Commons Attribution-Noncommercial-Share Alike 4.0 License](https://creativecommons.org/licenses/by-nc-sa/4.0/).

AN ABSTARCT OF THE CAPSTONE REPORT OF

Di An for the degree of Master of Chemical Sciences

Title: *Monolayer Self-Assembly of Monodisperse Nanocrystals at the Liquid-Air Interface*

Project conducted at: *University of Pennsylvania, Department of Chemistry, RM 337, Chem'73, 231 S. 34th Street, Philadelphia, PA 19104, USA*

Supervisor: *Christopher B. Murray, Richard Perry University Professor of Chemistry and Materials Science and Engineering*

Dates of Project: *May 15, 2019 – May 15, 2020*

Abstract approved:

Christopher B. Murray, Academic Advisor

The study of nanocrystals (NCs) self-assembly into monolayers have attracted significant interests, due to wide applications in sensors, catalysts, nanodevices and pattern transfer. Liquid-air interface self-assembly (LAISA) is a useful technique used for the monolayer fabrication. In this capstone project, a library of NCs is built for LAISA and binary superlattice study. Monodisperse iron oxide, gold and gadolinium fluoride NCs of various sizes were synthesized by modifying reported methods.^{9,10,20} The obtained NCs were characterized by TEM, SAXS, DLS and TGA, revealing their geometry, size and surface chemistry. The second part of this project is optimizing conditions of LAISA. Significant variables, including evaporation rate, NCs geometry, and ambient environment were isolated and studied for different building blocks. Centimeter-scale NCs monolayers with long-range order were obtained by using optimized conditions of LAISA. The binary superlattice system of spherical NCs was also investigated during this project with optimized LAISA. A 1:2 number ratio of iron oxide to gold NCs was used to fabricate binary superlattice monolayers by LAISA. The structure was revealed with TEM. However, future work is needed to investigate other size ratio and number ratio of two different kinds of NCs, and their effects on 2D structures.

*Monolayer Self-Assembly of Monodisperse
Nanocrystals at the Liquid-Air Interface*

by
Di An

A CAPSTONE REPORT

submitted to the

University of Pennsylvania

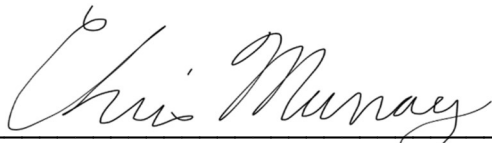
in partial fulfillment of
the requirements for
the degree of

Masters of Chemical Sciences

Presented April 28, 2020
Commencement *May 18, 2020*

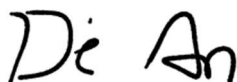
Master of Chemical Sciences Capstone Report of *Di An* presented on
(April 28, 2020)

APPROVED:



Prof. Christopher B. Murray, representing Inorganic Chemistry

I understand that my Capstone Report will become part of the permanent collection of the University of Pennsylvania Master of Chemical Sciences Program. My signature below authorizes release of my final report to any reader upon request.



Di An, Author

Acknowledgments

I sincerely appreciate my research advisor, Professor Christopher B. Murray for his guidance on my project and his helpful advices on my career. I acknowledge my mentor Austin W. Keller for helping me start my capstone project and taught me characterization and synthesis methods. I also give my thanks to Professor Zahra Fakhraai for her efforts and advice as my second reader. Special thanks to Dr. Ana-Rita Mayol-Cabassa as my program supervisor for her continuous support and kindness during my Master program. I also appreciate valuable support and cares from group members: Emanuele Marino, Shengsong Yang, Natalie Gogotsi, Daniel Rosen, Corbin Vara, Jennifer D. Lee, Katherine Elbert, Tianfan Jin, Xiang Zhou, Sjored van Dongen and Aditya Maan. I would also like to thank my parents for their support during my life, and my girlfriend's mental support in these two years.

Table of Contents

Abstract	i
Title Page	ii
Approval Page	iii
Acknowledgements	iv
List of Figures	vi
List of Appendices	vii
Introduction.....	1
Materials and Methods	4
Results and Discussion	9
Building blocks treatment and analysis	9
Self-assembly study and optimization	14
Binary superlattice system study	20
Conclusion.....	22
Future Work.....	22
References	24
Appendices.....	26

List of Figures

Figure 1. Demonstration of LAISA and Langmuir-Schaefer transfer.....	3
Figure 2. Iron-oleate precursor	4
Figure 3. TEM images of iron oxide from size selection	9
Figure 4. Iron oxide samples as building blocks and size analysis	10
Figure 5. Size selection on GdF ₃ @OA	11
Figure 6. TGA of as-synthesized and OA annealed iron oxide NCs	12
Figure 7. As-synthesized and OA annealed NCs in LAISA.....	13
Figure 8. SAXS and DLS analysis of iron oxide NCs.....	14
Figure 9. TEM images of 7.3 nm iron oxide NCs self-assembly with various solvent mixture ratio	15
Figure 10. TEM images of 3.8 nm iron oxide NCs self-assembly with various uncovered length	16
Figure 11. TEM images of concentration mapping	17
Figure 12. Ambient environment control	18
Figure 13. Subphase material survey	19
Figure 14. Geometry effect study and pattern transfer	20
Figure 15. Characterization of Au@DDT	21
Figure 16. Binary superlattice	22
Figure 17. Pattern transfer process	23

List of Appendices

Appendix 1. Iron Oxide Nanocrystals Library List.....	26
Appendix 2. Well-Ordered Monolayer and Bilayers.....	27

Introduction

Self-assembly is the spontaneous organization into ordered structures. This phenomenon happens both in nature and artificial forms. The self-assembly of nanocrystals (NCs) into monolayers is important and has attracted significant interests. Because of tunable optical and electronic properties,¹ monolayers of NCs have wide applications in catalysis,² sensors,³ electroluminescence devices⁴ and pattern transfer.⁵ Studying the self-assembly of NCs is meaningful for researchers to well understand the process of bottom-up fabrication, as well as to reveal the growth mechanism of 3D structures.⁶

Monodisperse NCs are defined as nanoparticles that have inorganic cores and uniformity in size, shape and surface chemistry with standard deviations no more than 5% in diameter, which are ideal building blocks for self-assembly.⁷ Synthesized NCs are usually grafted with organic molecular on the surface, termed ligands or capping groups.⁷ Surface ligands achieve the solubility of NCs in organic solvent, as well as tunable interparticle spacing. Spherical NCs such as iron oxide and gold NCs are good candidates for self-assembly study because of their tunable sizes and well-established synthesis methods.⁸⁻¹⁰ Apart from isotropic NCs that have a spherical shape, NCs such as gadolinium fluoride gain much attention because of the anisotropic geometry of rhombic plates.¹¹ The self-assembly of anisotropic NCs is interesting due to the different pattern of monolayers.

Iron oxide NCs with tunable sizes are important. Monolayers of iron oxide NCs have applications in nanodevices, and their magnetic properties are a function of particle sizes.¹² For pattern transfer application, tunable sizes of iron oxide make engineering the mask size possible. The self-assembly of two sizes of spherical NCs into binary superlattice structure has gain much attention in recent years, due to the many distinct structures NCs can form.¹³⁻¹⁵ The ability of tuning sizes is also important when studying the size ratio of iron oxide to gold NCs in binary superlattice system.

Self-assembly of NCs into 2D monolayers can take place on both solid and liquid substrates. For example, solid-air interface can be used for monolayer self-assembly.¹⁶ However, the surface of solid substrate is not perfect. NCs tend to aggregate at areas where there are defects, therefore degrading the quality of monolayers. The liquid-air interface self-assembly (LAISA) of NCs is preferred because NCs have more mobility than those at the solid surface. Therefore, NCs have more chances to adjust positions to form well-ordered 2D structures.¹⁷ The liquid phase is named as subphase, and it can be diethylene glycol (DEG)⁶ or deionized water.¹⁷ The choice of subphase influences the assembly process, because the surface tension is different and that can affect how NCs spread around.

The self-assembly techniques have been widely explored throughout the literature.^{6,17,18} However, fabricating monolayers that are well-ordered over large scale is still challenging. In reported studies, there are defects including grain boundaries¹⁸ and discontinuities¹⁹ of monolayers. There is also a lack of study of effects of ambient environment and how it should be controlled.

The first goal of this capstone project is to build a library of monodisperse building blocks that includes both isotropic and anisotropic NCs with different geometries and sizes for LAISA and binary superlattice monolayers study. To achieve this, spherical iron oxide and gold NCs with various diameters are synthesized as isotropic building blocks, while rhombic nanoplates of gadolinium fluoride NCs are synthesized as anisotropic building blocks. In previous report,⁸ monodisperse NCs of iron oxide were synthesized from iron-oleate precursor, which is from the reaction of iron pentacarbonyl and oleic acid. However, iron pentacarbonyl is toxic and expensive. In this project, iron oxide NCs can be synthesized from non-toxic and economic iron-oleate complex.⁹ Iron oxide NCs are synthesized with tunable diameters, achieved by changing the amount of ligands added during the synthesis. Monodisperse spherical gold NCs with the diameter of 5.0 nm are synthesized by modifying reported methods.¹⁰ Ligand exchange process is applied, enabling the substitution of oleylamine (OAm) with 1-dodecanethiol (DDT). Larger iron oxide NCs with a diameter of 7.3 nm and gold NCs with a diameter of 5.0 nm are used for binary superlattice study. The size of gold NCs is smaller, thus can be used to increase the interparticle spacing of iron oxide NCs. The binary superlattice system will be studied after the optimization of LAISA. Rhombic nanoplates of gadolinium fluoride are synthesized at high temperature by modifying the method reported by Paik.²⁰

The uniformity of NCs is important for self-assembly. In order to narrow down the size distribution, size selection procedure is adapted after the synthesis. The separation of NCs with different sizes is achieved by taking advantage of mass difference when centrifuged. Size selection yields monodisperse iron oxide NCs of 3.8, 7.3, 9.6 and 12.7 nm, representing small, medium and larger sizes. Surface ligand density should be improved to ensure the stability and mobility in solution. Improving NCs surface ligand density can be achieved by treating synthesized NCs with excess free ligands at a kinetically favorable temperature, termed annealing. The post-synthesis treatments of size selection and OA annealing are evaluated in this work.

Obtained NCs are characterized with TEM, SAXS and DLS, revealing morphology, inorganic core size and hydrodynamic size, respectively. Knowing inorganic core size can help accurately calculate the mass of the crystal core, without taking ligands into consideration. TGA is also used to confirm the effectiveness of ligand exchange on gold NCs, as well as to evaluate the annealing

process. The mass of individual NC can be used to determine size and number ratios of iron oxide to gold NCs for binary superlattice study.

The second goal is to optimize conditions of LAISA, and obtain large-scale, well-ordered NCs monolayers. This can be achieved by isolating important variables during LAISA and studying their influences individually. **Figure 1** shows a typical set up of LAISA. First a Teflon well with certain volume is cleaned and dried. Subphase material is then added into the well. The NCs are dispersed in organic solution and added onto the subphase in a dropwise manner. Because of the difference in surface tension between subphase and organic solvent, the NCs dispersion spreads over the surface of the subphase. The Teflon well is partially covered by a glass slide, making the evaporation rate higher at the uncovered side. Therefore, NCs move toward to the uncovered edge driven by drying force, forming monolayers (**Figure 1A**). Langmuir-Schaefer transfer method²¹ is used to transfer obtained monolayers onto a solid substrate (**Figure 1B**).

The key influencing factor is the evaporation rate of organic solvent used to disperse NCs. In order to achieve a moderate evaporation rate, organic solvent choice, uncovered length of Teflon well (l), and ambient environment will be studied and optimized (**Figure 1C**). The total number of NCs added is another important influencing factor of the quality of monolayers, which number is determined by the concentration and volume added of NCs dispersion. However, in order to ensure the efficiency of monolayers fabrication, the drying time should be controlled and should not be too long. When LAISA conditions are optimized, large-scale, well-ordered monolayers of different kinds of NCs and the binary superlattice system can be obtained and characterized with TEM.

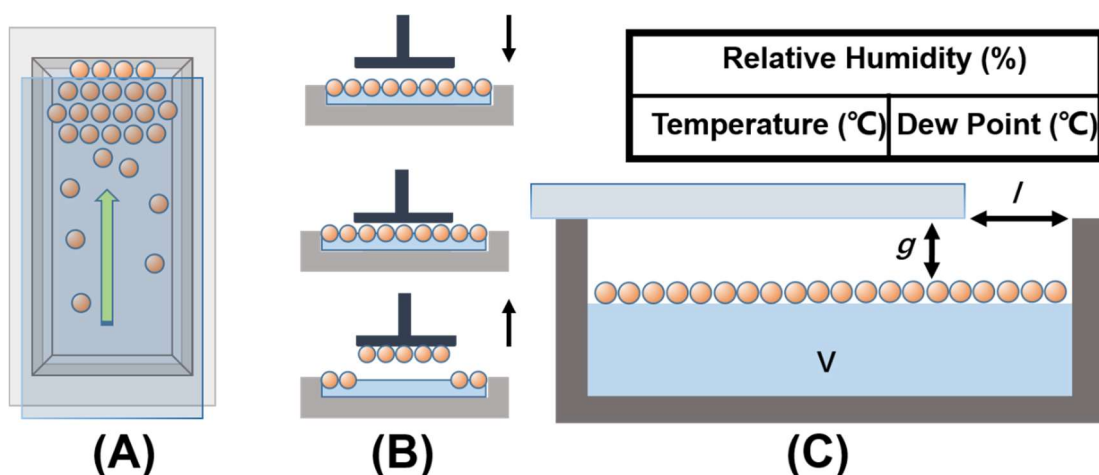


Figure 1. Demonstration of LAISA and Langmuir-Schaefer transfer. (A) The drying process of self-assembly (B) Langmuir-Schaefer transfer method. (C) Parameters of LAISA set up: subphase volume (V), air gap (g) and uncovered length (l).

Materials and Methods

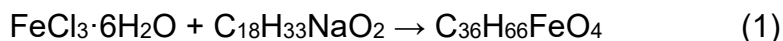
Materials

Triethylene glycol was purchased from Sigma-Aldrich and used without further purification. Ethylene glycol (99.5%), diethylene glycol (99%), tetraethylene glycol (99.5%) are purchased from Acros Organics and used as received. Gadolinium (III) oxide (99.99%), 1-octadecene (technical grade, 90%), oleic acid (OA, technical grade, 90%) and lithium fluoride (99.98%) were purchased from Sigma Aldrich and used as received. Iron chloride ($\text{FeCl}_3 \cdot 6\text{H}_2\text{O}$, 98%) is purchased from Aldrich and used as received. Sodium oleate (95%) is purchased from TCI and used as received. Hydrogen tetrachloroaurate (III) hydrate ($\text{HAuCl}_4 \cdot 3\text{H}_2\text{O}$, 99.0%), Oleylamine (OAm, 70%), 1,2,3,4-tetrahydronaphthalene (tetraline), tert-butylamine-borane (TBAB, 97%) and 1-dodecanethiol (DDT) are used as received without further purification.

Techniques

Iron Oxide NCs ($\text{Fe}_3\text{O}_4@OA$) Synthesis

First iron oleate precursor is prepared as follows: 10.8 g iron (III) chloride, 36.5 g sodium oleate, 40 mL DI water, 40 mL ethanol and 80 mL hexanes are added into a 250 mL three-neck flask. The reaction is described as **Equation 1**.



The mixture is refluxed at 60°C for 4 hours, generating a red-black color. Then the mixture is washed with DI water for three times in a separation flask. The obtained precursor is dried in a vacuum oven overnight at 70°C to remove remaining water (**Figure 2**).



Figure 2. Iron-oleate precursor.

Second, 7.2 g iron oleate precursor, 1.0 mL oleic acid (OA), and 20 mL 1-octadecene are added into a three-neck flask. The solution is then dehydrated under vacuum by a Schlenk line for 60 minutes at 110°C. The mixture is further heated to 315°C at a rate of 3°C/minute under nitrogen flow and kept at this temperature for 30 minutes. The mixture is then cooled in a water bath to stop the reaction. Third, every 5 mL mixture is washed with 5 mL toluene and 40 mL acetone. The mixture is centrifuged at 8000 ×g for 5 minutes. The precipitate is dissolved in toluene, and every 10 mL of the dispersion is washed with 10 mL ethanol and 30 mL isopropyl ethanol. The mixture is centrifuged at 8000 ×g for 5 minutes. The supernatant is discarded, and the precipitate is dissolved in toluene. 50 μL OA is added into the dispersion, which is then sonicated and vortexed. The second washing step is repeated and the precipitate is dried under vacuum. Stock solution of iron oxide with a diameter of around 10 nm is made by dissolving dried NCs in toluene.

Sub-5 nm iron oxide NCs with a diameter of 3.8 nm is obtained by modifying synthesis conditions as follows: in the second synthesis step, 1.25 mL OA is added, and the mixture is then heated to 95°C for 30 minutes. And the mixture is further heated to 290°C at a rate of 3°C/minute under nitrogen flow and kept at this temperature for 60 minutes. The same washing step is followed to make a stock solution of synthesized iron oxide NCs.

The volume added of OA, reaction temperature and time can affect the eventual size of iron oxide nanocrystals. Therefore, by changing the influencing factors, iron oxide nanocrystals of various diameters can be obtained. Because of the temperature fluctuation, diameters of NCs can be different from targeted sizes. A complete list of iron oxide NCs of different sizes can be found in **Appendix 1**.

Gold NCs (Au@DDT) Synthesis

Firstly, gold precursor is prepared by mixing 0.2 g HAuCl₄·3H₂O with 10 mL oleylamine (OAm) and 10 mL 1,2,3,4-tetrahydronaphthalene (tetraline) in a glass vial. The mixture is sonicated until all materials are dissolved well, which is then transferred carefully into a three-neck flask. The solution is stirred rigorously with nitrogen flowing, while the flask is set in ice water bath.

The second step is weigh 1 mmol tert-butylamine-borane (TBAB) and dissolve it in the mixture of 1 mL oleylamine and 1 mL tetraline. This solution is injected rapidly into the gold precursor. At least three hours are allowed for the growth of gold NCs.

Ligand exchange is conducted in a water bath set at 30°C. The reaction mixture is stirred rigorously when adding 1 mL 1-dodecanethiol (DDT). The length of DDT ligand is longer than OAm, stabilizing gold NCs. The reaction is run for 5 minutes, followed by washing steps.

The reaction solution is first washed with excess acetone, followed by centrifuge at 8000 ×g for 3 minutes. The precipitate is redispersed in hexane for the second washing step. Excess ethanol is added in the solution, which is then centrifuged at 8000 ×g for 3 minutes. The precipitate is dried under vacuum to remove residual solvent. Finally, hexane or chloroform can be used to dissolve obtained materials for storage, named Au@DDT.

Gadolinium Fluoride NCs (GdF₃@OA) Synthesis Procedure

Trifluoroacetate precursors is first prepared by mixing 10 g gadolinium (III) oxide, 50 mL trifluoroacetic acid and 50 mL DI H₂O in a 250 mL three-neck flask. The mixture is then refluxed at 80°C until the solution is clear, which is then dried under vacuum to get powder.

Nanoplates are synthesized by adding the mixture of 0.980 g Gd(CF₃COO)₃, 0.0257 g Er(CF₃COO)₃, 0.259 g Yb(CF₃COO)₃ and 0.216 g LiF into a 125 mL three-neck flask. A mixture solution of 30 mL OA and 30 mL 1-octadecene is then added into the flask. Schlenk line is used to provide vacuum environment for moisture and oxygen removal purpose. The degassing process is set at 125°C for 3 hours. The mixture is then heated to 290°C at a rate of 10°C/minute with nitrogen flow, and is kept at this temperature for 4 hours.

The synthesis is followed by washing steps to remove unreacted materials. The reaction mixture is washed with ethanol as antisolvent at a solvent to antisolvent ratio of 1:1. Then the solution is centrifuged at 6000 ×g for 2 minutes. The precipitate is then redispersed in hexane and washed with ethanol at a solvent to antisolvent ratio of 1:2, which is repeated twice. Finally, the precipitate is redispersed in hexane and centrifuged without antisolvent at 3000 ×g for 1 minute. Precipitate in the final washing step is discarded, and the supernatant is kept in a glass vial.

NCs Size Selection

Due to the fact that synthesized NCs are not always as monodisperse as desired, size selection⁷ process is usually conducted to narrow down the size distribution. NCs dispersed in nonpolar solvent, for example hexane, are first placed in a centrifuge tube. Dehydrated ethanol as antisolvent is added slowly in a dropwise manner into the solution. To ensure the antisolvent added is mixed well, it can be helpful to put a stir bar in the centrifuge tube and stir rapidly when adding antisolvent. With increasing antisolvent added, the solubility of NCs in this solution mixture is decreasing. This effect is more obvious for largest NCs. The adding of antisolvent should be ceased when the solution mixture looks cloudy, which means the solubility of large NCs is low enough. The solution mixture is then centrifuged, after which the supernatant is transferred into another centrifuge tube. This process is repeated until no precipitate presents after centrifuge. During the size

selection process, NCs precipitate in the order of sizes, from largest to smallest. Precipitation of NCs from each selection section can be redispersed in nonpolar solvent such as hexane and toluene, and then characterized by TEM.

Post-Synthesis Treatment: OA Annealing

The OA annealing process is adapted from work reported by Wang.¹³ Fe₃O₄@OA NCs are dispersed in toluene at a concentration of 5 mg/mL. For every milligram of NCs, 100 μ L OA is added and the mixture is stirred at 60°C for 24 hours. Ethanol is added into the mixture at a solvent to antisolvent ratio of 2:1 for washing purpose. The solution mixture is then centrifuged at 8000 \times g for 10 minutes. The supernatant is discarded while the precipitate is kept and dried under vacuum to remove residual solvent. NCs are re-dissolved in toluene at a concentration higher than 5 mg/mL for storage. The process can be repeated for as many as three times.

Liquid-Air Interface Self-Assembly.

LAISA experiments are completed in 2.25 \times 2.25 \times 1.0 cm³ Teflon wells. Subphase material (3.4 mL) is first added, filling about 75% volume of the Teflon well. Appropriate amount of NCs dispersion is then added onto the surface of subphase. Glass slides are used to cover Teflon wells fully or partially to achieve different evaporating rates of the organic solvent. In order to ensure a tight contact between glass slides and Teflon wells, glass vials filled with water are put on top of slides. A certain amount of drying time is allowed for the completed evaporation of organic solvent. Usually 60 mL octane can evaporate completely within 5 hours. In this project, effects of different drying time are studied.

Electron Microscopy.

All TEM images are taken at 120 kV voltage on a JEOL JEM-1400. TEM grids as solid substrates are used to take samples of monolayers.²² Samples are dried under vacuum to remove excess organic residue before characterization. The software ImageJ is used for TEM images processing to statistically analyze NCs size distributions.

Thermogravimetric analysis (TGA)

TGA is used to compare surface ligand density before and after annealing process by measuring mass loss of NCs. TGA analysis is conducted on TA instruments SDT-Q600. NCs in a powder form are heated from room temperature to 500°C at a heating rate of 25°C/minute. The temperature is held isothermally at 500°C for 5 minutes. Ligand exchange can be confirmed by running TGA on NCs and free ligand molecules. OA annealing process is evaluated by TGA by comparing the difference of mass loss.

Dynamic light scattering (DLS)

Hydrodynamic diameters of spherical NCs are measured with DLS technique. DLS measurement is completed on a Malvern Zetasizer Nano-ZS instrument. Glass cuvette with 1 cm path length is used with toluene as solvent. The measurement technique is the automatic 173° backscatter. By statistically analyzing raw data, equivalent hydrodynamic diameters can be obtained.

Small-angle X-ray scattering (SAXS)

SAXS data are collected by using a Pilatus 1M detector on a Xeus 2.0 system from Xenocs. The duration of each measurement is set for 30 minutes. Copper anode is used at 8 keV. The sample to detector distance is set as 1.2 m. Analysis software Sasfit is used to fit raw data to a sphere model. The mean radius and standard deviations are automatically given by the software.

Results and Discussion

Building Blocks Treatment and Analysis

Size Selection Evaluation

TEM is used to characterize the morphology and the images obtained are analyzed by ImageJ to analyze the size distribution. **Figure 3 (A-C)** shows TEM images of iron oxide NCs obtained from the first, second and third selection section, respectively. Size distribution analysis are presented in **Figure 3 (D-E)**, corresponding to each size selection section. The difference in sizes is obvious in **Figure 3A**, while it can be hardly observed in **Figure 3B** or **Figure 3C**. The size distribution is continually narrowed down by repeating size selection procedure, indicated by decreasing standard deviation of diameter from 3.2 to 1.0 nm (**Figure 3 D-F**). When the size selection is conducted for the third time, the size distribution of NCs has the mode of 7.1 nm with a standard deviation of 1.0 nm (**Figure 3F**), indicating NCs can be used as monodisperse building blocks for self-assembly.

Iron oxide NCs separated from each size selection step are not always too polydisperse to use as building blocks for self-assembly. Therefore, iron oxide NCs that have small standard deviations in diameters are kept in non-polar solvent for future study. The mode of size distribution is used as the size of NCs. A list of iron oxide NCs obtained from size selection can be found in **Appendix 1**. Smaller standard deviation is desirable, giving a low standard deviation to mean diameter ratio. A low ratio indicates NCs are monodisperse in size.

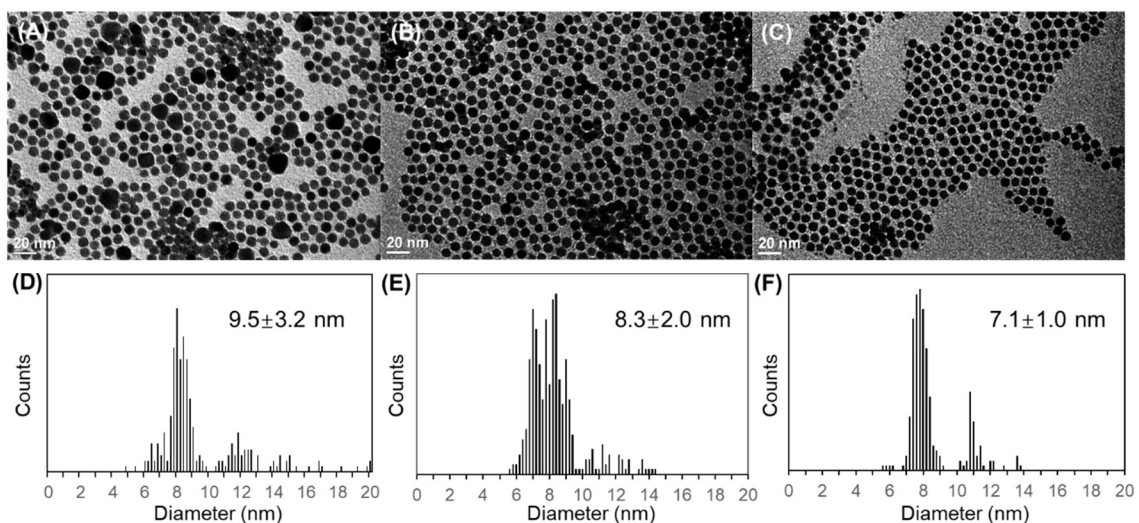


Figure 3. TEM images of iron oxide from size selection. NCs are from section 1 (A), section 2 (B), and section 3 (C) of size selection. Size distributions of NCs from each section are shown in (D), (E), and (F), respectively.

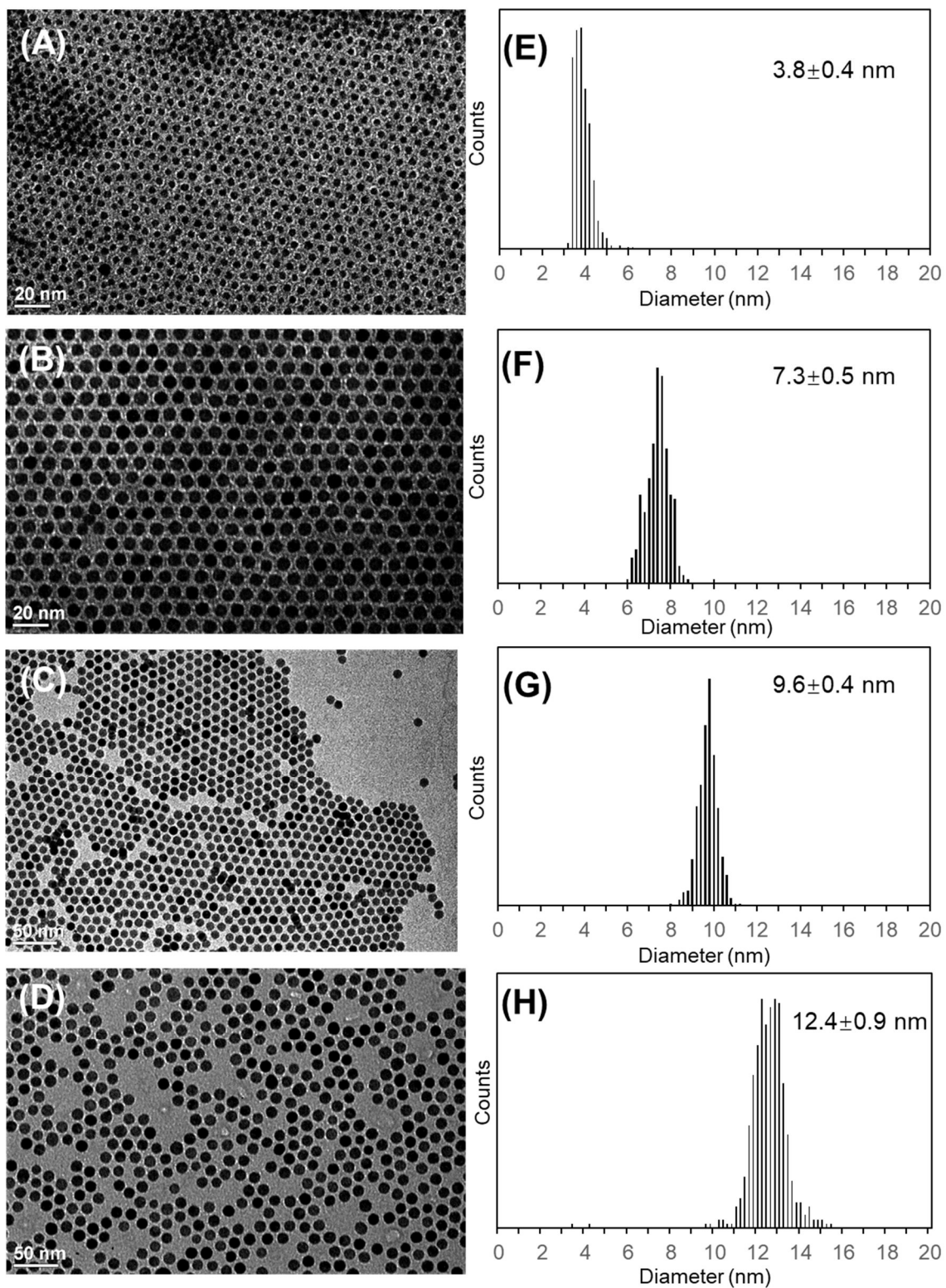


Figure 4. Iron oxide samples as building blocks and size analysis. Iron oxide NCs with average diameters of 3.8 nm (A), 7.3 nm (B), 9.6 nm (C), and 12.4 nm (D) are obtained.

The monodisperse iron oxide NCs used in this project are obtained by applying size selection. TEM images show that final samples are uniform in shape (**Figure 4 A-D**). The size distribution analysis is shown in **Figure 4 (E-H)**, with modes used as average diameters of 3.8 nm, 7.3 nm, 9.6 nm, and 12.4 nm. Small standard deviations also indicate a narrow size distribution. Therefore, iron oxide NCs from size selection procedure are considered as monodisperse, which are good building blocks for self-assembly study.

The size selection procedure is also effective on anisotropic NCs like rhombic nanoplates of gadolinium fluoride. The precipitate from each size selection section is redispersed in hexane, then characterized with TEM (**Figure 5 A-H**). Rhombic nanoplates are separated from smaller NCs during the first five sections, due to the larger mass (**Figure 5 A-E**). Smaller round NCs gradually precipitate during the last three sections of size selection (**Figure 5F-H**), when there is already a decent amount of ethanol as antisolvent in the solution. This way, fully grown nanoplates are separated from incompletely grown NCs.

The TEM images of GdF₃@OA NCs are analyzed with ImageJ to measure geometries of NCs. NCs with the smallest standard deviation are identified and used as anisotropic building blocks in LAISA study. The average long diagonal and short diagonal of the GdF₃@OA rhombic plates are 26.4 ± 1.2 nm and 16.6 ± 0.8 nm, respectively, with the thickness of 2.2 nm.

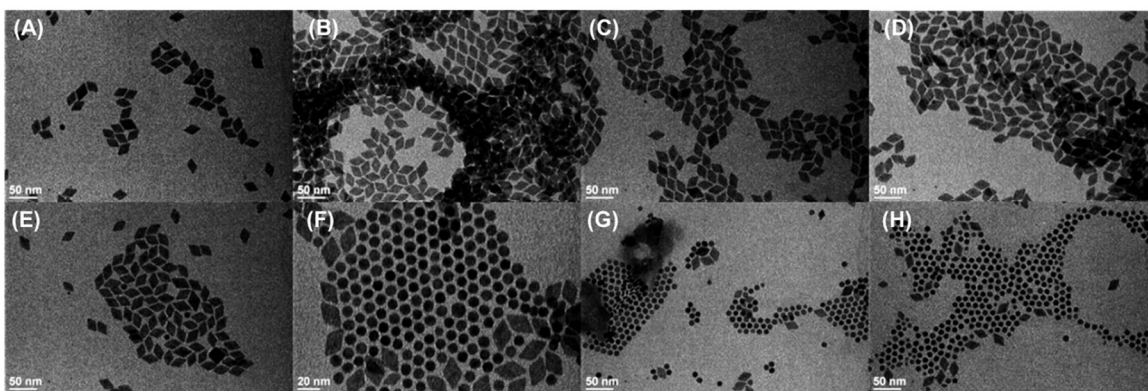


Figure 5. Size selection on GdF₃@OA. A-H are TEM images from each section of the size selection process in a time order.

Post-Synthesis Treatment: OA Annealing

OA annealing¹⁶ can be performed on NCs as a post-synthesis treatment to improve the surface density of ligands. TGA is used to measure mass loss of NCs during the heating, which is attributed to ligands loss.

The change of remaining weight of NCs is indicated by weight loss curves in **Figure 6A**. The TGA of free OA shows the temperature at which the loss of surface ligands begins noticeable is at around 180°C (**Figure 6B**). As-synthesized and OA annealed NCs also begin to loss mass at around 180°C, indicated by the black

and red weight loss curves respectively (**Figure 6A**). Therefore, the loss of mass for two samples can be attributed to the loss of surface ligand. The uneven change of slopes in (**Figure 6A**) is possibly due to instrument error, imperfect sample preparation or the energy barrier that surface ligands have to overcome. The ending point of black line is at 82.8%, which is 3.2% higher than that of red line at 79.6%. The difference of 3.2% weight between as-synthesized and OA annealed NCs confirms that OA annealing treatment improved the density of surface ligands. The remaining weight is attributed to inorganic cores.

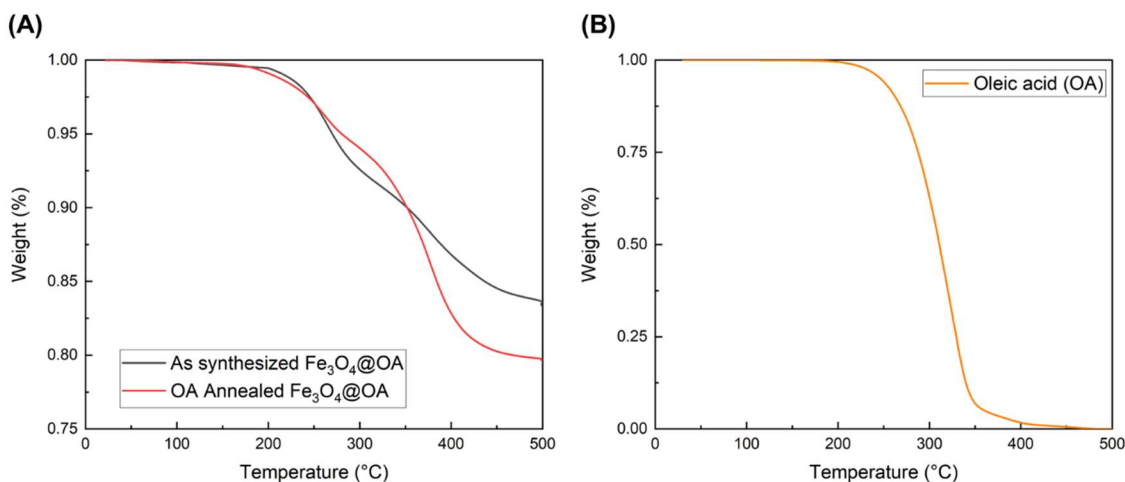


Figure 6. TGA of as-synthesized and OA annealed iron oxide NCs. (A) remaining weight percent versus temperature. (B) remaining weight percent of free OA versus temperature.

As-synthesized and OA annealed 7.3 nm iron oxide NCs are used for self-assembly to study the effect of surface ligand density on the quality of monolayer. Both NCs samples are dispersed in octane at a concentration of 0.4 mg/mL. The LAISA experiments are run overnight to ensure fully evaporation of solvent. Films are transferred onto TEM grids and then characterized.

By comparing self-assembly results, it can be found that the OA annealed NCs can improve the overall quality of monolayers. **Figure 7 A** and **B** are TEM images of OA annealed NCs assembly, compared with assemblies obtained by using as-synthesized NCs (**Figure 7 C&D**). During the assembly, OA annealed NCs tend to spread on the subphase surface, due to a higher surface ligand density. **Figure 7 B** and **D** indicate that bilayers are less likely to appear from annealed NCs, compared with films formed from as-synthesized NCs.

The magnified images of monolayer regions also prove that OA annealed iron oxide NCs can achieve a long-range, close-packed order (**Figure 7B**). While the monolayer of as-synthesized suffers from defects of discontinuity and vacancies (**Figure 7D**).

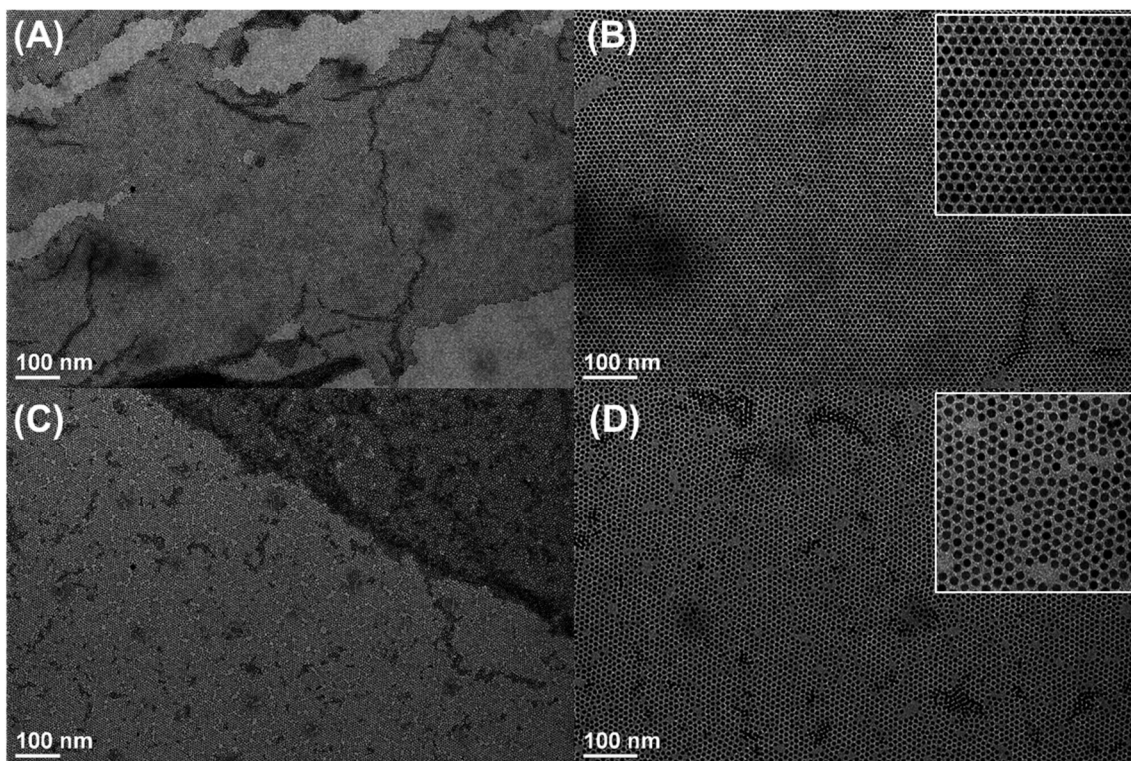


Figure 7. As-synthesized and OA annealed NCs for LAISA. (A) monolayer of OA annealed NCs. (C) monolayer of as-synthesized NCs. (B) and (D) are magnified images showing packing structure, with respect to (A) and (C).

Size Analysis with SAXS and DLS

It is important to know the inorganic core size when calculating the mass of individual NC. The hydrodynamic diameters of OA capped NCs are significant when analyzing effective diameters of NCs in monolayer. Therefore, the inorganic core size and hydrodynamic diameter of NCs are measured with SAXS and DLS, respectively. The inorganic core diameters of iron oxide NCs can be obtained from fitting the raw SAXS data (red dots in **Figure 8 A-C**) to spherical model (solid lines in **Figure 8 A-C**). Diameters can be estimated based on fitting curves from Sasfit software, giving 8.2 ± 0.6 nm, 10.3 ± 0.6 nm, 13.2 ± 1.0 nm, with respect to **Figure 8 A, B&C**. During the measurement, scattering intensity is recorded versus scattering vector (q). The diameters of spherical samples can also be estimated from the value of scattering vector at the first minimum (q_{firstmin}). Hydrodynamic diameters of iron oxide NCs in toluene are measured by DLS. Results show the intensity curves versus sizes. Maxima of curves are hydrodynamic diameters of NCs, giving 11.7, 15.7 and 18.2 nm (**Figure 8D**). Hydrodynamic diameters are larger than sizes measured by SAXS, because ligand length is included when using DLS technique. It can also be found in **Figure 8D** that curves are narrow, indicating they are monodisperse building blocks that are good for LAISA study.

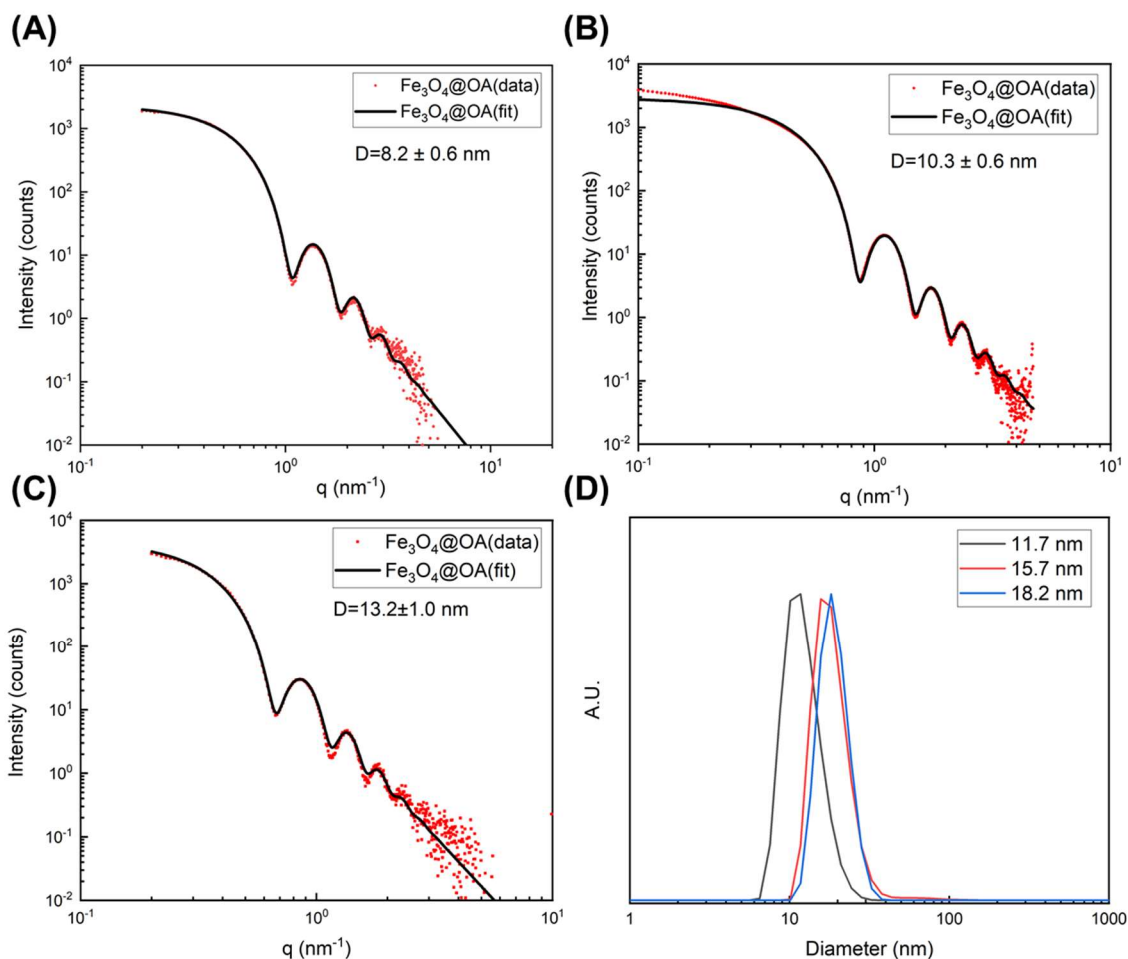


Figure 8. SAXS and DLS analysis of iron oxide NCs. The fit curve gives diameters of 8.2 ± 0.6 nm (A), 10.3 ± 0.6 nm (B), 13.2 ± 1.0 nm (C). Hydrodynamic diameters are shown in DLS analysis (D).

Self-Assembly Study and Optimization

Solvent Choice Study

Solvent choice is an important variable in LAISA. Solvent with a low boiling point, such as hexane, leads to a fast evaporation, usually generating multiple-layers of NCs at the interface. Mixing hexane with less volatile solvent can achieve a moderate evaporation rate. Octane, with a boiling point of 125°C , can be mixed with hexane as a solvent mixture for NCs dispersion. The effect of solvent mixture ratio is studied. The amount of octane in the solvent mixture is set at 100%, 95%, 75% and 50%, where 100% octane means no hexane is added. Concentration and volume added are kept as constant at 0.4 mg/mL and 55 μL . All Teflon wells are fully covered and allowed for 3 hours drying. Corresponding results are shown in **Figure 9**. The TEM image color is a function of thickness. Electrons have longer path length at thicker regions, resulting darker color. The light grey tone in **Figure**

9A represents monolayer area, while the darker color represents multilayers that are thicker. The magnified TEM image at the top-right corner shows the order at monolayer area. Pure octane has the lowest evaporation rate, thus achieves large area of monolayer, corresponding to the light grey area in **Figure 9A**. When 10% hexane is added, the solvent mixture evaporates faster than pure octane, forming bilayers mainly, revealed by black regions in **Figure 9B**. The magnified TEM image shows the structure of NCs bilayers. With larger component of hexane in the solvent mixture, the evaporation rate is higher, resulting in multiple-layers of NCs that are indicated by increasingly darker color in TEM images (**Figures 9 C&D**). There is still small amount of monolayers formed at higher evaporation rates, indicated by the lightest grey color in **Figure 9C** and **Figure 9D**. While films are mainly bilayers and thicker multiplayers, indicated by increasingly darker color in **Figure 9C** and **D**. The magnified images at the right-top corner in **Figure 9C** and **D** show the monolayer structure at the lightest color regions.

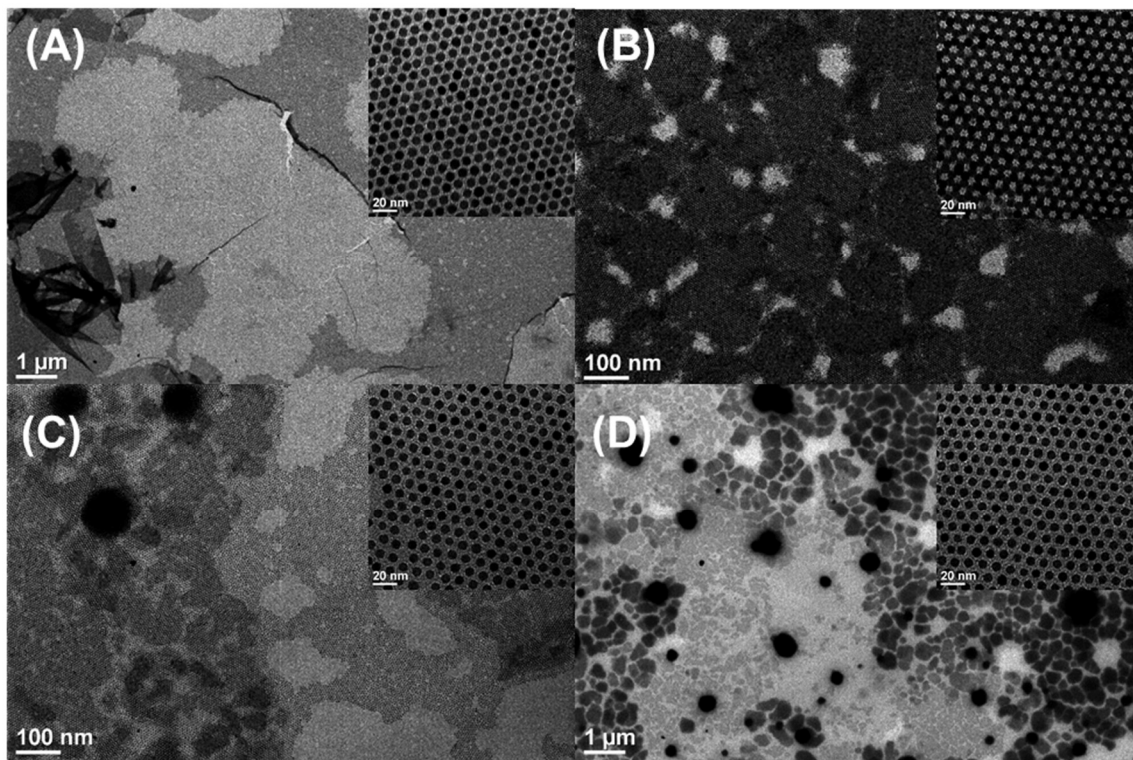


Figure 9. TEM images of 7.3 nm iron oxide NCs self-assembly with various solvent mixture ratio. The octane to hexane ratio is 9:1 (B), 3:1 (C), and 1:1 (D), while (A) is pure octane.

Uncover Length of Teflon Well Optimization

Solvent mixture mapping shows that pure octane as solvent is reasonable to achieve monolayer of NCs domains. However, the uncovered length of Teflon well also greatly influences the evaporation rate of solvent. In order to determine an appropriate uncovered length, a set of comparison LAISA experiments are conducted, with pure octane as solvent. Iron oxide NCs with the average diameter of 3.8 nm are used in octane at a concentration of 0.2 mg/mL.

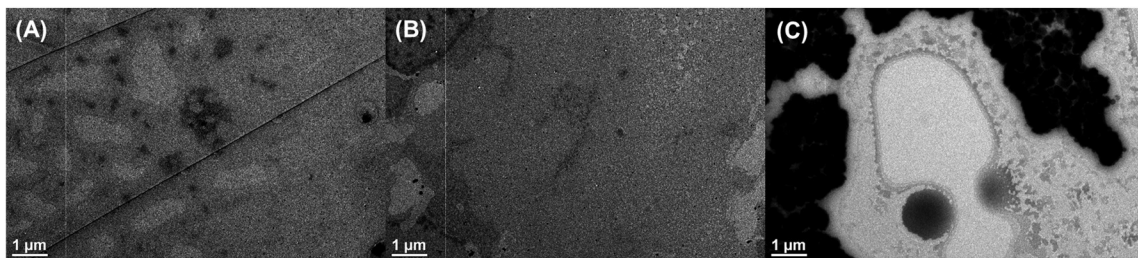


Figure 10. TEM images of 3.8 nm iron oxide NCs self-assembly with various uncover length. The uncovered percentages of Teflon well are 0% (A), 3% (B) and 5% (C).

Figure 10 shows TEM images of NCs films obtained using LAISA technique, with respect to different uncovered percentage of Teflon well. The uncovered percentage can be determined by calculating the ratio of uncovered length to total length. It can be found that with 0% (**Figure 10A**) and 3% (**Figure 10B**) uncovered length, the films obtained are mainly monolayers, indicated by grey color, while the lightest color represents vacuum. Thicker films form occasionally, indicated by darker color in **Figure 10A** and **Figure 10B**, because there is no significant driving force to cause the motion of NCs at a certain direction. This can be found by using high magnification. However, low magnification images are more helpful to reveal the coverage of monolayer over micrometer scale. When the Teflon well is 5% uncovered, aggregation happens, resulting in NCs islands that are shown by black domains in **Figure 10C**. This phenomenon is because that NCs tend to move towards the uncovered side faster at a high evaporation rate. Solvent evaporates before NCs have a chance to spread and adjust positions.

NCs Concentration Mapping

In LAISA, the total number of NCs added should be controlled below the number of NCs needed to cover the entire subphase surface. Concentration mapping helps to find an interval that yields monolayer. Iron oxide NCs with an average diameter of 3.8 nm are dispersed in octane at various concentrations at 0.1, 0.15, 0.2 and 0.4 mg/mL for self-assembly. Teflon wells are 3% uncovered and the drying time is 3 hours. TEM images of assemblies are shown in **Figure 11**.

Figure 11 A&B show discontinuity and vacancy of the monolayers, represented by the lightest color that indicates vacuum. Defects happen because the number of NCs is not sufficient to cover the surface. With concentration increased to 0.2 mg/mL, the contrast of TEM images (**Figure 11C**) is even over micrometer scale, confirming the continuous monolayer. The magnified image reveals the ordered structure (**Figure 11C**). The quality of monolayer is improved because there are sufficient NCs. If the concentration is further increased to 0.4 mg/mL, bilayers begin to form, represented by dark lines that appear in **Figure 11D**. Therefore, excess amount of NCs should be avoided.

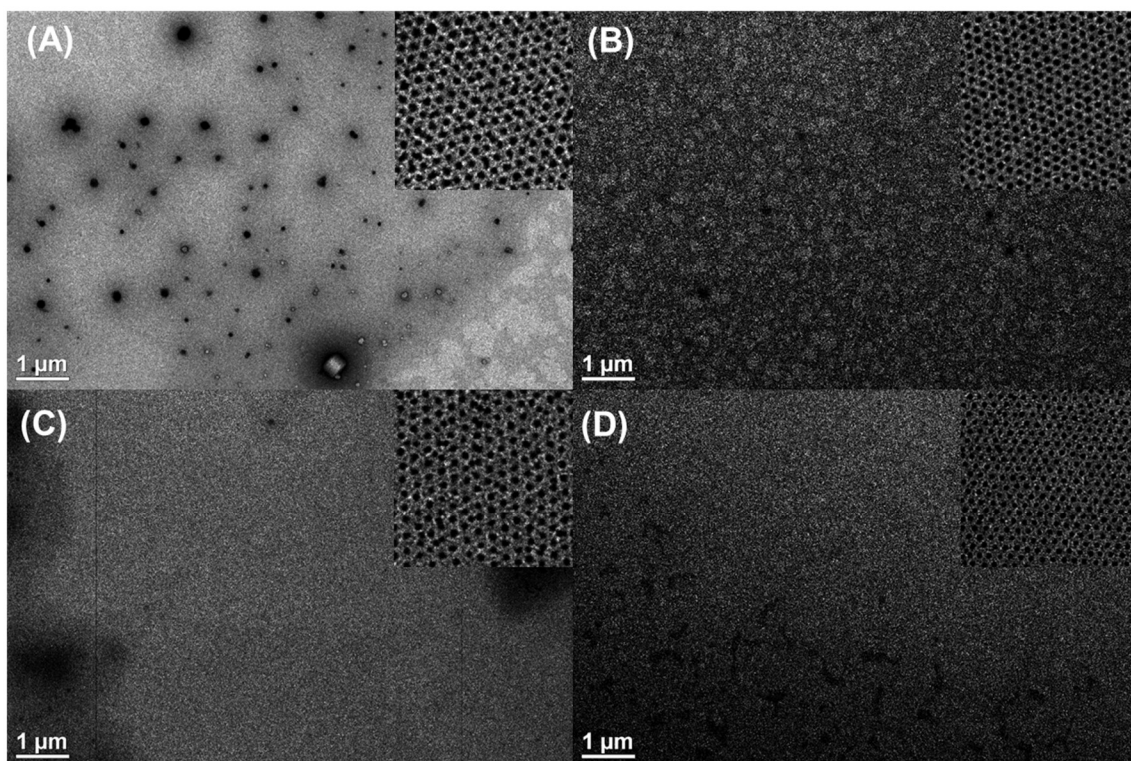


Figure 11. TEM images of concentration mapping. The concentrations of iron oxide NCs dispersion are 0.1, 0.15, 0.2 and 0.4 mg/mL, with respect to A, B, C and D.

Ambient Environment Control

The temperature is stable at about 22°C in the room where LAISA are conducted. However, the relative humidity can change from 12% to as high as 50%. It is necessary to maintain a stable humidity level when conducting LAISA, because it can significantly influence the evaporation rate of organic solvent. A glovebox is used to achieve controllable ambient environment, by setting a water source inside the box, as shown in **Figure 12D**. The relative humidity in this glovebox can be maintained between 30% to 50%, which help to moderate

evaporation rate. **Figure 12C** is the picture captured by a phone camera to show the scale of iron oxide NCs monolayer, which is in the order of centimeter. The monolayer is hard for human eyes to see clearly, due to the small size of this iron oxide NCs used, which is 7.3 nm in diameter. Sample of the monolayer is taken with TEM grids for characterization. **Figure 12A** and **B** are TEM images taken at low and high magnification, showing the scale and structure of the monolayer, respectively. The contrast in **Figure 12A** is even, meaning the continuous monolayer. There are black dots distributed in **Figure 12A** as well. However, high magnification image **Figure 12B** confirms that the film is monolayer with close-packed order. Therefore, the black dots in **Figure 12A** can be attributed to residual organic matter. To conclude, with the relative humidity maintained at a high level of around 50%, the coverage of subphase surface is in centimeter scale, while the long-range close-packed order structure is still reserved. Iron oxide NCs are dispersed in octane at 0.3 mg/mL, added dropwise and allowed to dry overnight, with the Teflon well fully covered. Optimized LAISA is used to fabricate monolayers of iron oxide NCs with various diameters. TEM images of assemblies can be found in **Appendix 2**.

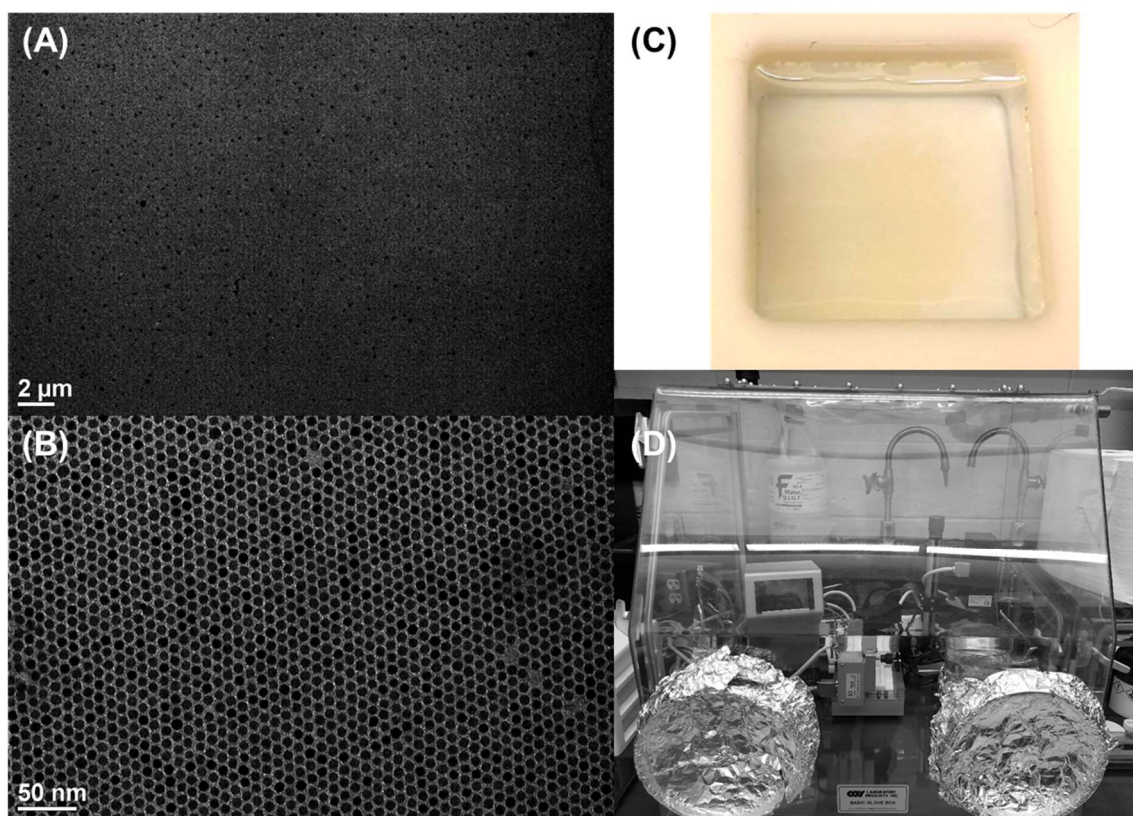


Figure 12. Ambient environment control. TEM images of self-assembly in this glovebox under low (A) and high (B) magnification show the scale and order of monolayer. (C) picture of LAISA. (D) glovebox used to control humidity.

Geometry Effect Study

The geometry of NCs used as building blocks affect the pattern of monolayer. Rhombic nanoplates of OA capped gadolinium fluoride NCs ($\text{GdF}_3\text{@OA}$) are used as anisotropic building blocks in LAISA to study the effect of geometry. Due the anisotropic geometry, a survey of subphase material is conducted because DEG may not support nanoplates as well as spherical NCs. The LAISA experiments of $\text{GdF}_3\text{@OA}$ are run on EG, DEG, TriEG and TetraEG. $\text{GdF}_3\text{@OA}$ NCs are likely to stack on each other to form multilayers on DEG (**Figure 13B**), TriEG (**Figure 13C**) and TetraEG (**Figure 13D**) subphase, indicated by overlapping parts under TEM. While on EG (**Figure 13A**) $\text{GdF}_3\text{@OA}$ NCs can spread over the surface to form the monolayer. Therefore, EG is used as subphase material for $\text{GdF}_3\text{@OA}$ LAISA.

Using optimized conditions of LAISA, the monolayer of $\text{GdF}_3\text{@OA}$ is obtained. TEM images taken at low, medium and high magnification are shown in **Figure 14 A-C**. The area of monolayer is in the order of several micrometers (**Figure 14A**). While it is noticed that the pattern is different from that formed by iron oxide NCs, due to the isotropic geometry of gadolinium fluoride NCs (**Figure 14C**). The image taken at medium magnification (**Figure 14B**) confirms that the ordered structure is maintained over long range. The monolayer of $\text{GdF}_3\text{@OA}$ can be transferred on solid substrates: such as wafer or TEM grids, and used as a mask. The pattern can be reserved on substrates after applying etching procedure and the removal of NCs mask (**Figure 14D**).

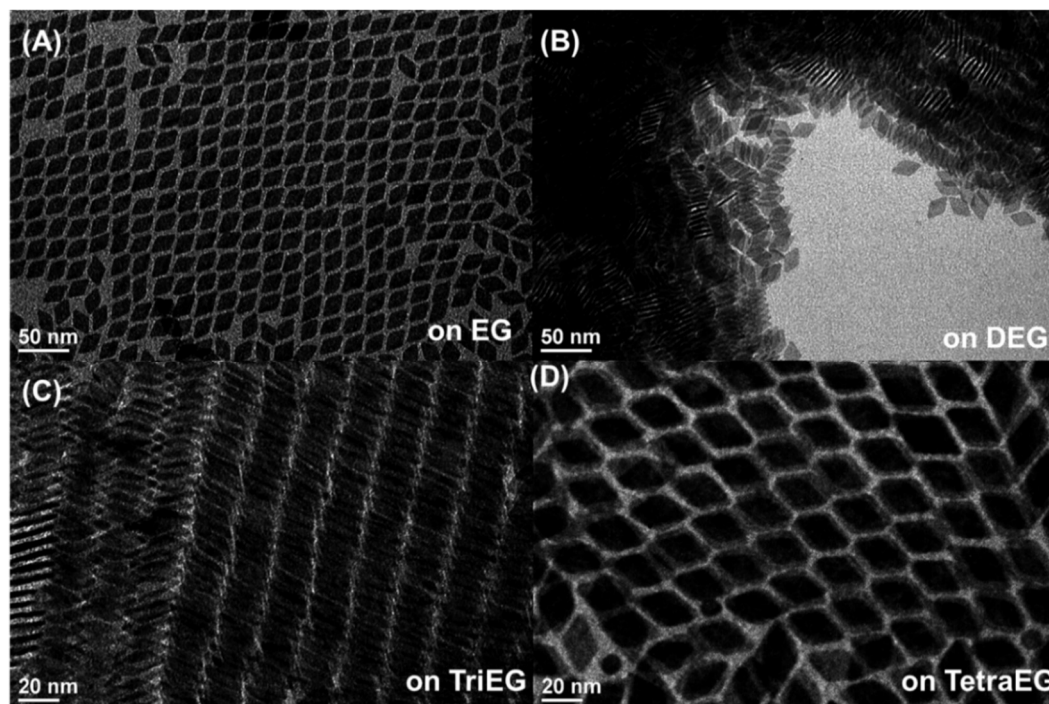


Figure 13. Subphase material survey. LAISA on different kinds of subphases: (A)EG, (B)DEG, (C)TriEG, (D) TetraEG.

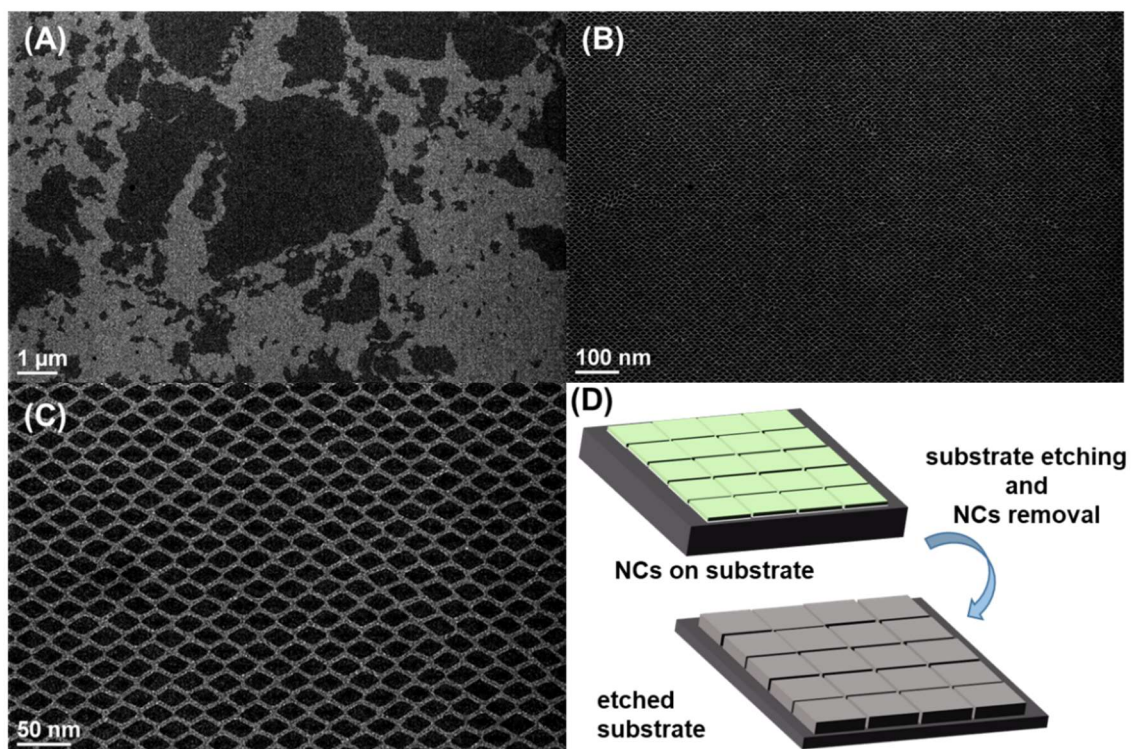


Figure 14. Geometry effect study and pattern transfer. (A), (B) and (C) TEM images from low magnification to high. (D) Pattern transfer demonstration.

Binary Superlattice System Study

The TEM image analysis of Au@DDT is shown in **Figure 15A**, giving the diameter of 5.2 ± 0.3 nm. The standard deviation of 0.3 nm means a narrow size distribution. SAXS and DLS analysis give inorganic core size and hydrodynamic diameter. The SAXS data (yellow dots in **Figure 15B**) is fitted to a sphere model, represented by solid red line in **C**. The diameter of 4.8 ± 0.3 nm can be estimated from the first minimum of fitted curve from Sasfit software. The maxima of DLS curve gives the hydrodynamic diameter of 10.1 nm (**Figure 15C**). DLS takes the length of surface ligand into consideration, resulting in a larger size than the inorganic core alone. TGA in **Figure 15D** shows that free DDT begins to lose mass at about 125°C, and stops at around 260°C. While the starting and ending of mass loss for Au@DDT are at about 215°C and 290°C, respectively. The temperature changes of Au@DDT NCs show a delay both at starting and ending points, which can be explained by the energy barrier that surface ligands have to overcome before thermal decomposition. TGA test confirms the success of ligand exchange on gold NCs. The weight loss curve of Au@DDT stops at 89.2%, indicating the crystal core makes up 89.2% of total mass.

Knowing the actual inorganic core sizes of iron oxide and gold NCs can help make accurate calculation of the mass and number ratio. Based on SAXS measurement, the diameters ratio of iron oxide to gold NCs is 10.3:4.8. The

number ratio of iron oxide to gold NCs is set at 1:2. The NCs mixture is dispersed in octane. The monolayer of this binary superlattice is obtained with LAISA on DEG.

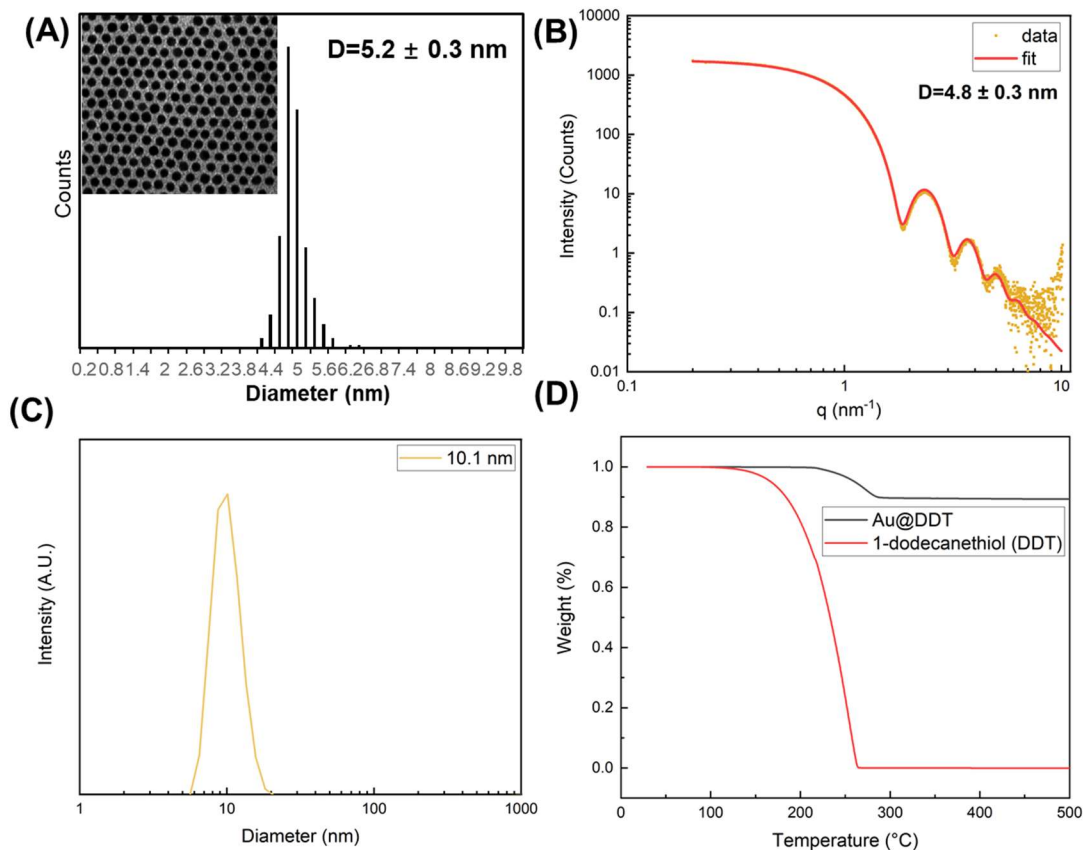


Figure 15. Characterization of Au@DDT. (A) TEM image and size distribution, (B) SAXS data and fit curve, (C) DLS analysis and (D) TGA.

Figure 16 shows TEM images of binary superlattice monolayers obtained by LAISA. Different concentrations of NCs solution yield different 2D structures. The monolayer shown in **Figure 16 A** and **B** is from 0.4 mg/mL NCs solution, with a distorted AIB₂ structure from literature.¹⁴ The model of 2D structure reveal the local order (**Figure 16C**). It can be found that iron oxide NCs are positioned in lines, which is due to this particular size ratio. When 0.8 mg/mL NCs solution is used, an AB type structure forms locally (**Figure 16D&E**). The model of this 2D structure in **Figure 16F** shows the position relationship between iron oxide and gold NCs. However, it is believed that different structures should not be solely attributed to concentration difference. Future work is needed to understand size and number ratios effect on structures. The binary superlattice LAISA also needs further optimization, in order to extend local order to larger area.

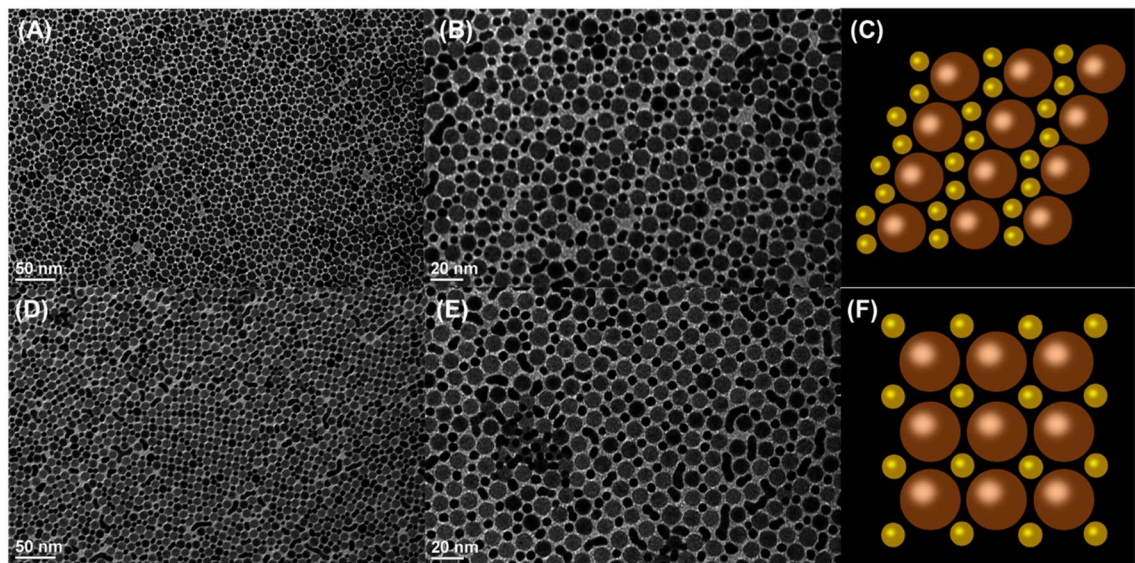


Figure 16. Binary superlattice. TEM images of monolayer by using NCs at 0.4 mg/mL (A) and 0.8 mg/mL (D) and structure models (C&F).

Conclusion

In conclusion, a library of monodisperse NCs as building blocks has been built for self-assembly and binary superlattice study. Spherical iron oxide and gold NCs with various diameters were synthesized as isotropic building blocks. Rhombic gadolinium fluoride nanoplates were prepared as anisotropic building blocks. NCs were treated with excess ligands after size selection procedure. TEM, SAXS and DLS were used to measure important parameters of NCs, including morphology, inorganic core and hydrodynamics sizes. TGA was used to evaluate the effectiveness of ligand exchange and OA annealing. The evaporation rate control was achieved by optimizing key variables including solvent choice, uncovered length of Teflon well and ambient environment. Centimeter-scale monolayers of iron oxide NCs were fabricated successfully using optimized LAISA technique. Gadolinium fluoride NCs were fabricated into monolayer with a different pattern over micrometer-scale area. Gold NCs were used as the second component in the binary superlattice system for the study of size ratio and number ratio influences on 2D structures.

Future Work

Octane has been used as non-polar solvent for NCs dispersion. There are potential choices of less volatile solvent for NCs dispersion. Toluene is non-polar solvent with a boiling point of 110.6°C. Volatile solvent such as hexane and chloroform can be used to mix with toluene,⁹ in order to achieve a desired evaporation rate. The volume ratio of the solvent mixture can be explored further to enrich choices of solvent. The self-assembly of gadolinium fluoride nanoplates

can be further optimized by trying different solvent mixture, with the goal of achieve centimeter-scale monolayer with ordered structure reserved.

Ligand exchange can also be applied on iron oxide NCs, in order to tune interparticle spacing of iron oxide NCs monolayer. Polystyrene and dendrimer are good candidates, due to the longer length of molecule.

With the library of iron oxide and gold NCs ready, the effect of number ratio and size ratio of two different kinds of NCs can be further investigated. There is a large number of combinations of different sizes iron oxide and gold NCs.¹⁶⁻¹⁸

The obtained ordered monolayer at the liquid-air interface can be transferred onto wafer for pattern transfer study.⁵ The concept is shown in **Figure 17**. The NCs monolayer can be transferred on solid substrate and used as a mask (**Figure 17A**). Substrate between NCs is etch (**Figure 17B**). After the removal of NCs by wet chemistry method, the pattern of monolayer is reserved (**Figure 17C**). The top-down perspective can help to understand the pattern of substrate. The engineering of mask size is made possible, with various sizes of iron oxide NCs. The binary superlattice monolayer can also be used as mask for pattern transfer, where gold NCs are used to tune interparticle spacing and relative position of iron oxide NCs.

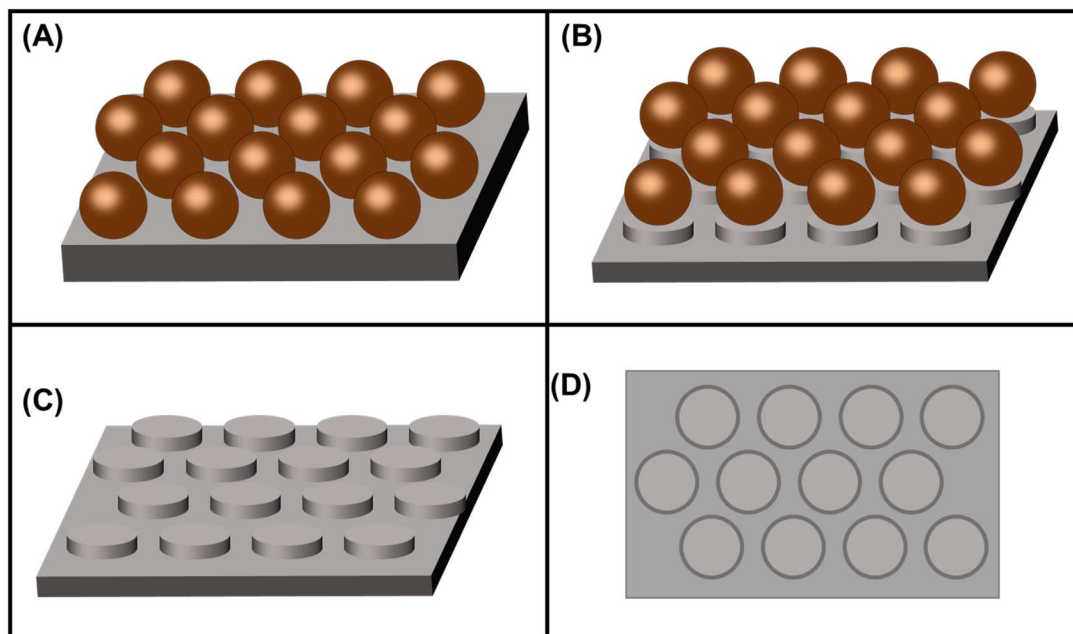


Figure 17. Pattern transfer process. (A) NCs monolayer as the mask. (B) etching on substrate. (C) NCs removal. (D) Top-down view of final result.

References

- (1) Yang, G.; Hu, L.; Keiper, T. D.; Xiong, P.; Hallinan, D. T. Gold Nanoparticles Monolayers with tunable Optical and Electrical Properties. *Langmuir*. **2016**, *32*, 4022-4033.
- (2) Yu, C.; Guo, X.; Muzzio, M.; Seto, C.T. ; Sun, S. Self-Assembly of Nanoparticles into Two-Dimensional Arrays for Catalytic Applications. *ChemPhysChem*. **2019**, *20*, 23-30.
- (3) Shipway, A. N.; Katz, E.; Willner, I. Nanoparticle Arrays on Surfaces for Electronic, Optical, and Sensor Applications. *ChemPhysChem*. **2000**, *1*, 18–52.
- (4) Coe, S.; Woo, W. K.; Bawendi, M.; Bulovic, V. Electroluminescence from Single Monolayers of Nanocrystals in Molecular Organic Devices. *Nature*. **2002**, *420*, 800–803.
- (5) Hogg, C. R.; Picard, Y. N.; Narasimhan, A.; Bain, J. A.; Majetich, S. A. Pattern Transfer with Stabilized Nanoparticles Etch Masks. *Nanotechnology*. **2013**, *24*, 085303.
- (6) Dong, A.; Ye, X.; Chen, J.; Murray, C. B. Two-Dimensional Binary and Ternary Nanocrystals Superlattices: The Case of Monolayers and Bilayers. *Nano Lett*. **2011**, *11*, 1804-1809.
- (7) Murray, C. B.; Kagan, C. R.; Bawendi, M. G. Synthesis and Characterization of Monodispersed Nanocrystals and Close-Packed Nanocrystals Assemblies. *Annu. Rev. Mater. Sci*. **2000**, *30*, 545-610.
- (8) Hyeon, T.; Lee, S. S.; Park, J.; Chung, Y.; Na, H. B. Synthesis of Highly Crystalline and Monodisperse Maghemite Nanocrystallites without a Size-Selection Process. *J. Am. Chem. Soc*. **2001**, *123*, 12798–12801.
- (9) Park, J.; An, K.; Hwang, Y.; Park, J.; Noh, H.; Kim, J.; Park, J.; Hwang, N.; Hyeon, T. Ultra-Large-Scale Syntheses of Monodisperse Nanocrystals. *Nat. Mater*. **2004**, *3*, 891-895.
- (10) Cargnello, M.; Johnston-Peck, A. C.; Diroll, B. T.; Wong, E.; Datta, B.; Damodhar, D.; Doan-Nguyen, V. V.; Herzing, A. A.; Kagan, C. R.; Murray, C. B. Substitutional Doping in Nanocrystal Superlattices. *Nature*. **2015**, *524*, 450-454.
- (11) Elbert, K. C.; Vo, T.; Krook, N. M.; Zygmunt, W.; Parl, J.; Yager, K. G.; Composto, R. J.; Glotzer, S. C.; Murray, C. B. Dendrimer Ligand Directed Nanoplate Assembly. *ACS Nano*. **2019**, *13*, 14241-14251.
- (12) Wang, Y.; Wei, W.; Maspoch, D.; Wu, J.; Dravid, V. P.; Mirkin, C. A. Superparamagnetic Sub-5 nm Fe@C Nanoparticles: Isolation, Structure, Magnetic Properties, and Directed Assembly. *Nano Lett*. **2008**, *8*, 3761-3765.
- (13) Wang, P.; Qiao, Q.; Zhu, Y.; Ouyang, M. Colloidal Binary Supracrystals with Tunable Structural Lattices. *J. Am. Chem. Soc*. **2018**, *140*, 9095-9098.

- (14) Coropceanu, I.; Boles, M. A.; Talapin, D. V. Systematic Mapping of Binary Nanocrystal Superlattices: The Role of Topology in Phase Selection. *J. Am. Chem. Soc.* **2019**, *141*, 5728-5740.
- (15) Udayabhaskararao, T.; Altantzis, T.; Houben, L.; Coronado-Puchau, M.; Langer, J.; Popovitz-Biro, R.; Liz-Marzan, L. M.; Vukovic, Lela.; Kral, P.; Bals, S.; Klajn, R. Tunable Porous Nanoallotropes Prepared by Post-Assembly Etching of Binary Nanoparticle Superlattices. *Science*. **2017**, *358*, 514-518.
- (16) Lin, X. M.; Jaeger, H. M.; Sorensen, C. M.; Klabunde, K. J. Formation of Long-Range-Ordered Nanocrystal Superlattices on Silicon Nitride Substrates. *J. Phys. Chem. B.* **2001**, *105*, 3353-3357.
- (17) Wen, T.; Majetich, S. A. Ultra-Large-Area Self-Assembled Monolayers of Nanoparticles. *ACS nano*. **2011**, *5*, 8868-8876.
- (18) Dong, A.; Chen, J.; Vora, P. M.; Kikkawa, J. M.; Murray, C. B. Binary Nanocrystal Superlattice Membranes Self-Assembled at the Liquid-Air Interface. *Nature*. **2010**, *466*, 474-477.
- (19) Bigioni, T. P.; Lin, X. M.; Nguyen, T. T.; Corwin, E. I.; Witten, T. A.; Jaeger, H. M. Kinetically Driven Self Assembly of Highly Ordered Nanoparticle Monolayers. *Nat. Mater.* **2006**, *5*, 265–270.
- (20) Paik, T.; Ko, D.; Gordon, T. R.; Doan-Nguyen, V.; Murray, C. B. Studies of Liquid Crystalline Self-Assembly of GdF₃ Nanoplates by In-Plane, Out-of-Plane SAXS. *ACS*. **2011**, *5*, 8322-8330.
- (21) Langmuir, I.; Schaefer, V. J. Activities of Urease and Pepsin Monolayers. *J. Am. Chem. Soc.* **1938**, *60*, 1351–1360.
- (22) Santhanam, V.; Liu, J.; Agarwal, R.; Andres, R. P.; Self-Assembly of Uniform Monolayer Arrays of Nanoparticles. *Langmuir*. **2003**, *19*, 7881-7887.

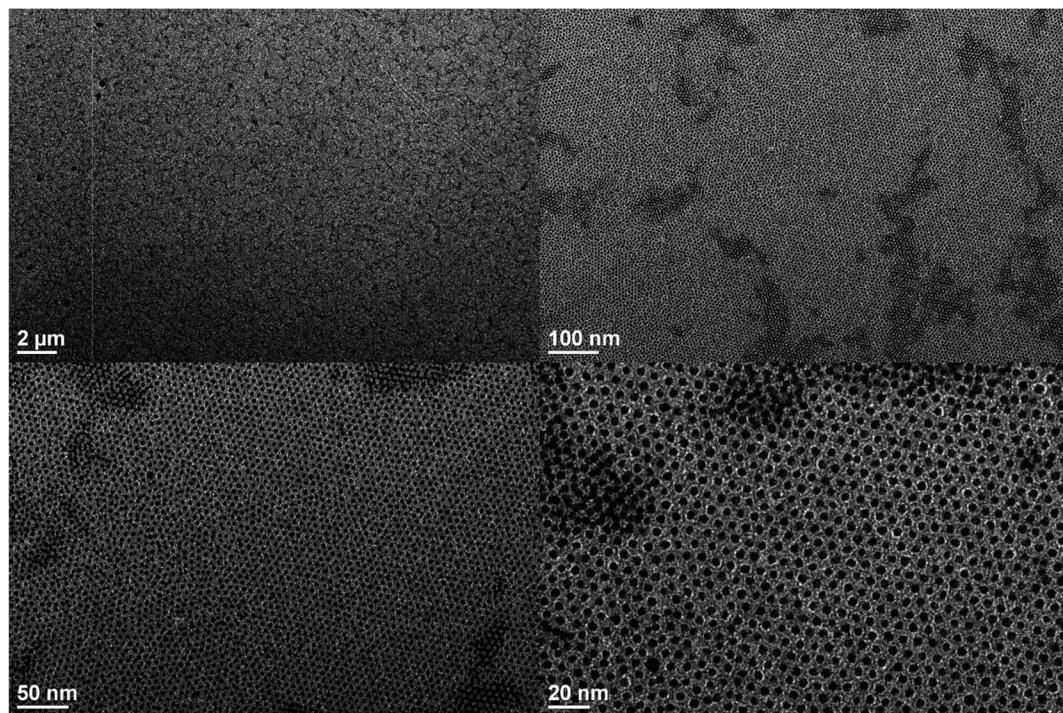
Appendices

Appendix 1. Iron Oxide Nanocrystals Library List

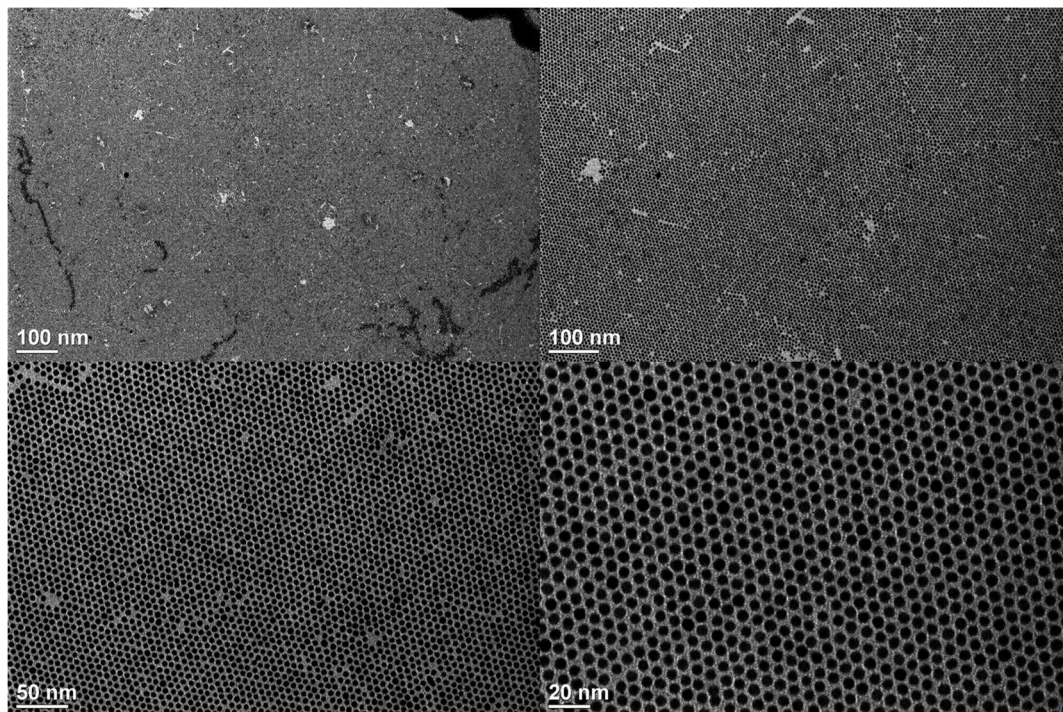
Sample Number	Mean (nm)	STDEV.P (nm)
#1 Fe ₃ O ₄ @OA	6.8	1.2
#2 Fe ₃ O ₄ @OA	7.0	1.7
#3 Fe ₃ O ₄ @OA	7.3	0.5
#4 Fe ₃ O ₄ @OA	7.9	0.8
#5 Fe ₃ O ₄ @OA	8.2	2.2
#6 Fe ₃ O ₄ @OA	8.2	1.5
#7 Fe ₃ O ₄ @OA	8.6	1.0
#8 Fe ₃ O ₄ @OA	8.8	1.2
#9 Fe ₃ O ₄ @OA	9.0	0.5
#10 Fe ₃ O ₄ @OA	9.4	1.4
#11 Fe ₃ O ₄ @OA	9.6	0.4
#12 Fe ₃ O ₄ @OA	9.9	1.1
#13 Fe ₃ O ₄ @OA	10.7	2.5
#14 Fe ₃ O ₄ @OA	12.4	0.7
#15 Fe ₃ O ₄ @OA	12.7	0.9

Appendix 2. Well-Ordered Monolayer and Bilayers

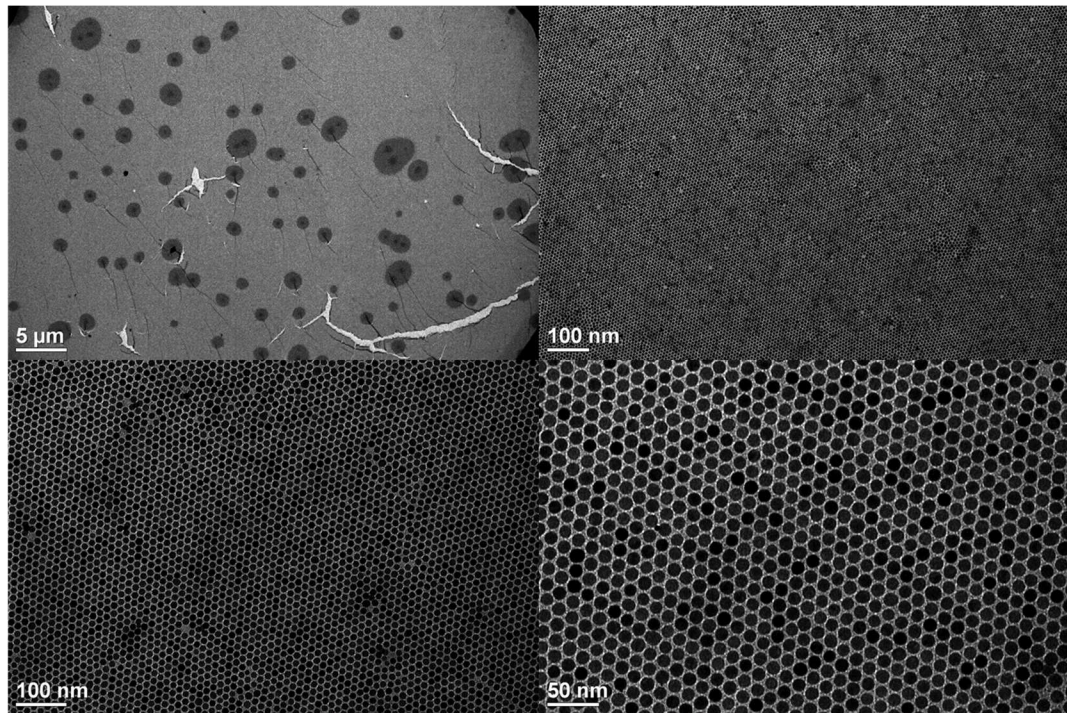
The 3.8 nm iron oxide monolayer:



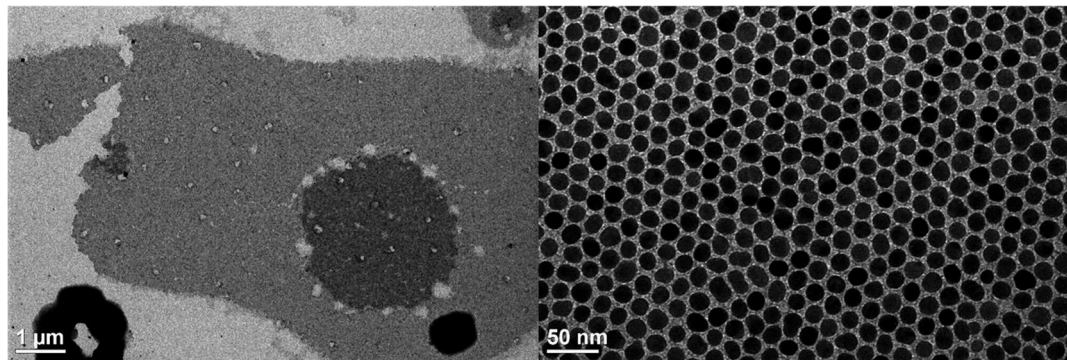
The Au@DDT monolayer:



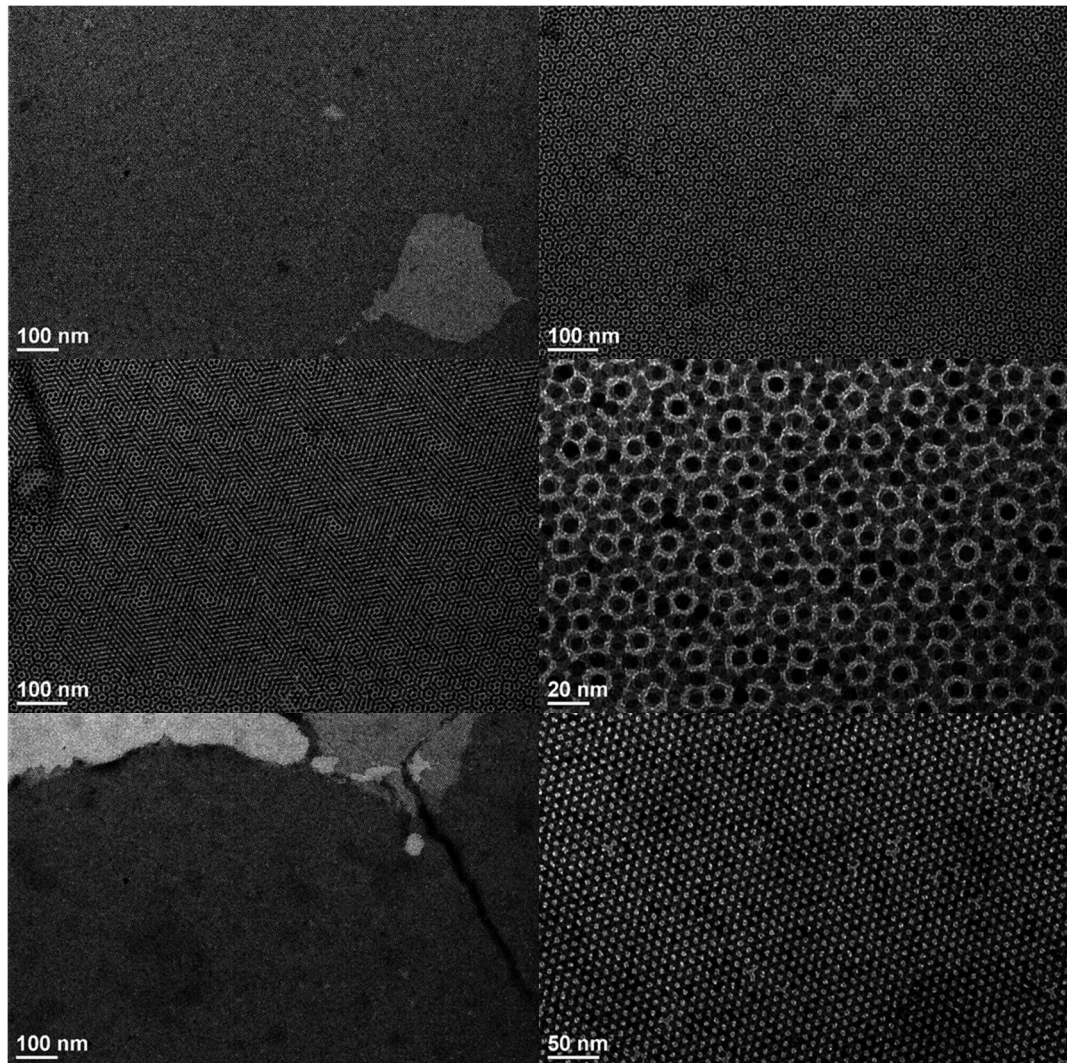
The 12.7 nm iron oxide monolayer:



The 17.0 nm iron oxide monolayer:



Bilayer of 7.3 nm iron oxide:



Well-ordered gadolinium fluoride monolayer:

